Simulation of Day-Length Encoding in the SCN: From Single-Cell to Tissue-Level Organization

Jos Rohling,[*,†] Lex Wolters,[†] and Johanna H. Meijer[*,1]

[*]*Department of Molecular Cell Biology, Group Neurophysiology, Leiden University Medical Center, Leiden, The Netherlands,* [†]*Leiden Institute of Advanced Computer Science, Leiden University, Leiden, The Netherlands*

Abstract   The circadian pacemaker of the SCN is a heterogeneous structure containing many single-cell oscillators that display phase differences in gene expression and electrical activity rhythms. Thus far, it is unknown how single neurons contribute to the population signal measured from the SCN. The authors used single-unit electrical activity rhythms that have previously been recorded in SCN slices and investigated in simulation studies how changes in pattern shape and distribution of single neurons alter the ensemble activity rhythm of the SCN. The results were compared with recorded ensemble rhythms. The simulations show that single units should be distributed in phase to render the recorded multiunit waveform and that different distributions can account for the multiunit pattern of the SCN, including a bimodal distribution. Vice versa, the authors show that the single-unit distribution cannot be inferred from the ensemble pattern. Photoperiodic encoding by the SCN relies on changes in waveform of the neuronal output from the SCN and received special attention in this study's simulations. The authors show that a broadening or narrowing of the multiunit pattern can be based on changes in phase differences between neurons, as well as on changes in the circadian pattern of individual neurons. However, these mechanisms give rise to differences in the maximal discharge level of the multiunit pattern, leading to testable predictions to distinguish between the 2 mechanisms. If single units broaden their activity pattern in long days, the maximum frequency of the multiunit activity should increase, while an increase in phase difference between the single-unit activity rhythms should lead to a decrement in maximum frequency. The simulations also show that coding for day-length by an evening and morning oscillator is not self-evident and will only work under a limited set of conditions in which the distribution within each component and temporal distance between the components is taken into account. While the simulations were based on single-cell and multiunit electrical activity patterns, they are also relevant for understanding the relation between single-cell and population molecular expression profiles.

Key words   circadian rhythms, suprachiasmatic nucleus, entrainment, photoperiodic encoding, evening/morning oscillators, simulation

---

A major pacemaker for circadian rhythms in mammals is located in the SCN of the anterior hypothalamus. Individual neurons of the SCN have a genetic basis for rhythm generation, which is explained by a transcriptional-translational feedback loop of clock genes and protein products. When dissociated or measured in cultures, with little synaptic connectivity, SCN neurons continue to be rhythmic in electrical activity, transmitter release, and gene expression and show a range of circadian periods (Welsh et al., 1995; Herzog et al., 2004; Honma et al., 2004; Shinohara et al., 1995; Watanabe et al., 1993). In a network (or slice), cells synchronize, resulting in a peak in electrical activity at midday and a trough during the night. Recordings in slices have shown that exposure to long and short days modifies the waveform of the multiunit activity pattern of the SCN in rats and hamsters (Schaap et al., 2003; Mrugala et al., 2000; Sumova et al., 1995; Jac et al., 2000; Schwartz et al., 2001). In a short day, the peaks in a multiunit activity pattern are narrow, while in a long day, the peaks are wider. The studies did not reveal whether the changes in multiunit pattern reflected a similar change in the waveform of individual neuronal discharge rhythms.

We have previously recorded circadian rhythms in electrical impulse frequency in single-unit and subpopulation activity in the rat SCN in hypothalamic slices and observed that single units have short durations of increased electrical activity and show maximum frequency levels at various phases of the circadian cycle (Schaap et al., 2003). We concluded that the accumulated activity of the single units accounts for the neuronal ensemble pattern of the SCN, indicating that circadian waveform of electrical activity is a tissue property. Brown et al. (2005) confirmed that single units have short durations as compared to the ensemble pattern of the SCN. For gene expression rhythms, Quintero et al. (2003) and Yamaguchi et al. (2003) found phase differences in the oscillations in Per1, indicating that phase differences may also occur in gene expression cycles.

Although several studies have shown that the single units are distributed in phase, it is still unknown how the units are distributed over the circadian cycle and whether different environmental conditions (i.e., long and short day-lengths) lead to changes in phase distribution. In this article, we performed simulations of SCN multiunit activity based on single-unit recordings (Schaap et al., 2003) and investigated how changes in distribution among oscillating neurons affect the recorded multiunit activity pattern. While we previously explored changes in a linear distribution between neurons (Schaap et al., 2003), we now explore different distributions (normal and bimodal distribution) with different parameter settings (i.e., σ and the temporal distance between 2 peaks in a bimodal distribution) and investigated the outcome of these changes for the multiunit pattern. In addition, we explored whether a broadening or narrowing of the single-cell activity patterns themselves leads to changes in multiunit activity patterns. This last issue is especially interesting in understanding whether coding for day-length can occur at the single cell level or may require a neuronal network. The present simulations did not aim to mathematically describe coupling mechanisms between the neurons. Our major objective was to show how different distributions between neurons and changes in single-unit activity patterns affect the multiunit pattern. These changes may play a role in the ability of the circadian system to adapt to changes in the environment, both on a daily and a seasonal basis. This article includes counterintuitive findings and presents testable predictions. Moreover, it shows the usefulness of simulations based on single-cell oscillators to obtain insight in the multioscillator structure of the SCN.

MATERIALS AND METHODS

The simulations were aimed to evaluate the contribution of single-clock neurons to the overall electrical output of the mammalian circadian pacemaker. Simulation software was implemented in Matlab, a high-level technical computing language and interactive environment. The simulations involved calculation of the multiunit activity pattern from single-unit activity patterns. The multiunit activity pattern was simulated by distributing single-unit activity patterns over the circadian cycle and then adding up the equally weighted activity of all single units. The intrinsic parameters of the simulation were the shape and width of the activity pattern of the single unit, the type of the distribution, the phase difference of the single-unit patterns over the cycle, and the number of single units that constitute the multiunit pattern. We investigated the effects of parameter changes on the width of the multiunit activity pattern at the half-maximum amplitude (cf. Schaap et al., 2003). The amplitude of the simulated multiunit patterns was normalized to enable qualitative predictions, except for Figure 5, where quantitative changes in population pattern were examined. The results were compared with multiunit patterns recorded under 3 different photoperiods: short

day-length (LD 8:16), normal day-length (LD 12:12), and long day-length (LD 16:8). The single-unit pattern as well as the distribution could independently be narrowed or broadened. The results could be graphically presented with or without photoperiod indication, single units, and an indicator of the width of the pattern.

For these simulations, an approximation of a single-unit activity pattern was given by using an average pattern of 9 previously measured single units of the rat SCN (Schaap et al., 2003). These units had been recorded in acutely prepared slices with stationary electrodes from animals that were kept in a 12:12-h light-dark cycle. The mean circadian activity pattern of these neurons was calculated by normalizing the activity pattern of each neuron. The peaks of the normalized signals were placed on top of each other to determine the mean circadian waveform for an SCN neuron. The pattern shows an abrupt onset of activity, which could be artifactual. Although we cannot exclude this, the average waveform is the best estimation of a single-unit pattern available to our knowledge.

We used 4 different distributions in our simulations: a linear, normal, bimodal, and trimodal distribution. The linear distribution was used in Schaap et al. (2003) and spreads the single-unit activity patterns linearly over the light period, with the peak of the first unit at light onset and the peak of the last unit at light offset (see Fig. 1D). In the normal or Gaussian distribution, the single-unit activity patterns were normally distributed over a certain time window within the circadian cycle, where the Gaussian distribution was characterized by $e^{-(x-\mu)^2/2\sigma^2}/(\sigma*\sqrt{2\pi})$ (see Fig. 1E). The distribution used in our simulation is not a proper Gaussian distribution, but its tails are cut off as we deal with a repetitive signal with a period of 24 h. The σ could be changed from low values (narrow distribution) to high values (broad distribution). A bimodal distribution was used to simulate evening and morning oscillators (see Fig. 1F). This distribution has 2 components, and each of them was given either a Gaussian or a linear distribution. The first component was set around light onset and the second component around light offset. The distance between the components, measured in hours, as well as the distribution within the components could be manipulated. The trimodal distribution obtained an additional component at midday.

To account for changes in multiunit activity patterns that occur through seasonal changes, simulations were performed to investigate waveform changes in 3 different photoperiods. We investigated the effects of
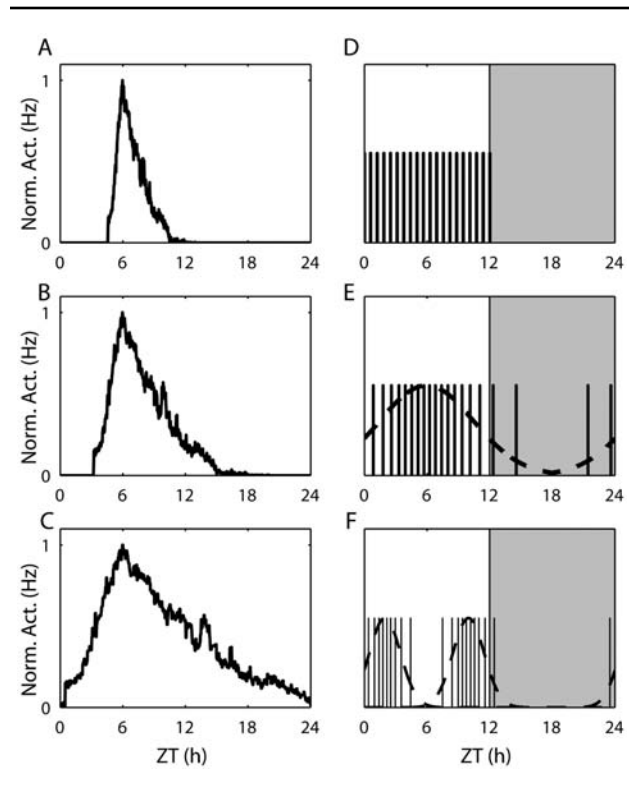

Figure 1.   Single-unit activity patterns and distributions. (A) A narrow single-unit activity pattern, (B) a measured single-unit activity pattern, and (C) a broad single-unit activity pattern. The measured pattern is the average from 9 recorded single-unit activity patterns. Patterns A and C are derived from the measured pattern B by modifying it to half or to twice its width. The maximum frequency of each pattern is normalized and is set to ZT6. (D-F) Different distributions of peak times of single units. (D) A linear distribution in a normal photoperiod (LD 12:12). (E) A normal distribution over a 24-h period. (F) A bimodal distribution with means at ZT2 and ZT10.

changing the phase relation between the single units in the linear, normal, or bimodal distribution on the width of the multiunit pattern. In addition, we investigated the outcome of changes in single-unit activity patterns. A change in waveform of single-unit activity patterns was achieved by narrowing the width by half or broadening it 2-fold (see Figs. 1 A-C). In addition, the effects of a range of widths of single-unit activity patterns on the multiunit pattern were investigated.

RESULTS

From Single-Cell to Multiunit Pattern

We simulated multiunit patterns from measured single-unit patterns that either were or were not distributed over the circadian cycle. When the single

units are not distributed and are all active at the same time, the obtained multiunit pattern is narrow (Fig. 2A). When, on the other hand, single units are distributed in phase, a broader multiunit activity pattern is obtained (Fig. 2B). This broader pattern resembles the multiunit activity pattern that is measured with stationary electrodes in slices (Fig. 2C). To investigate the influence of the number of recorded neurons on the multiunit activity pattern, we varied the number of neurons in the simulation. At first, an arbitrary number of 10 single-unit activity patterns were distributed over the day (Fig. 3A). This results in a multiunit activity pattern with a width of 13.12 h, which is similar to data from slice recordings, although there are more fluctuations in the signal. An increase in the number of units renders a smoother multiunit activity pattern that becomes slightly more narrow (Figs. 3 A-C).

Different distributions of single-unit activity patterns can all lead to multiunit activity patterns that resemble recorded patterns. A Gaussian distribution ($\sigma = 180$) results in a multiunit activity pattern with a width of 12.21 h (Fig. 3D). A bimodal distribution, with the mid of the first component at ZT3 and the mid of the second component at ZT9 (each with $\sigma = 135$), renders a peak width of 12.05 h (Fig. 3E). Finally, a trimodal distribution with the mid of the 3 components at ZT2, ZT6, and ZT10 (each with $\sigma = 135$) renders a peak width of 12.38 h (Fig. 3F). We conclude that for all distributions, solutions exist that lead to a realistic multiunit pattern.

It appeared difficult to predict the underlying distribution of single units on the basis of the recorded multiunit activity pattern (Figs. 3, 4). A bimodal distribution of single units can result in a bimodal multiunit pattern, if the peaks are at ZT3 and ZT9 (Fig. 4A) and if the distribution within each component is rather narrow. It can also result in a unimodal multiunit pattern if the peaks are closer together (i.e., at ZT4 and ZT8; Fig. 4B) or if the distribution within each component is broader. A bimodal multiunit pattern can also be obtained by an underlying distribution of 3 subpopulations (Fig. 4C).

Mechanisms for Photoperiodic Encoding

It is well known that a multiunit pattern is narrow in a short photoperiod and broadens when the photoperiod increases (Jagota et al., 2000; Schaap et al., 2003). We investigated whether changes in the width of multiunit patterns can result from changes in the width of single-unit patterns (Fig. 5A). For a linear
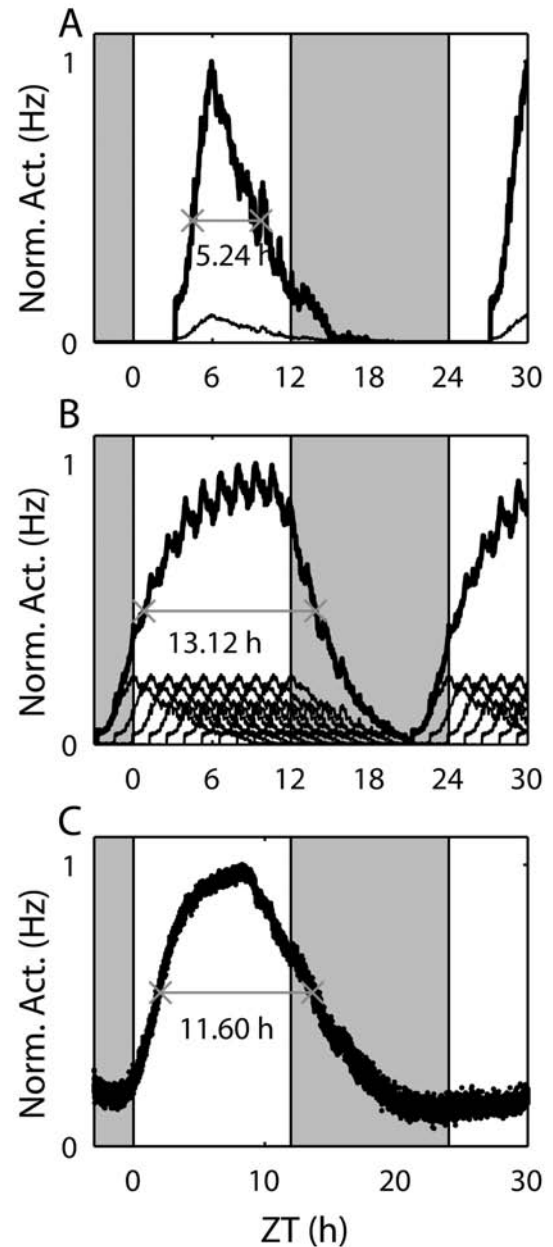

Figure 2. **Multiunit activity pattern recording and simulation based on the single-unit activity patterns as used in Figure 1B. (A) Single-unit patterns with their peaks in electrical activity at the same time (ZT6). An added multiunit pattern of an arbitrary number of 10 neurons is shown. The single-unit patterns are indicated at the bottom. The resulting multiunit pattern is narrow as compared to the recorded pattern of C. (B) Single-unit patterns distributed over the light period. The added multiunit pattern of an arbitrary number of 10 neurons that are linearly distributed over the light period is shown, with the single units indicated at the bottom. The resulting multiunit pattern broadens and resembles the recorded activity pattern. (C) Example of a multiunit pattern in the rat SCN slice recorded with a stationary electrode. Slices were acutely prepared from rats kept in LD 12:12. The simulated multiunit pattern can be compared to the measured patterns with respect to the width, which is measured at the half-maximum level of the pattern.**
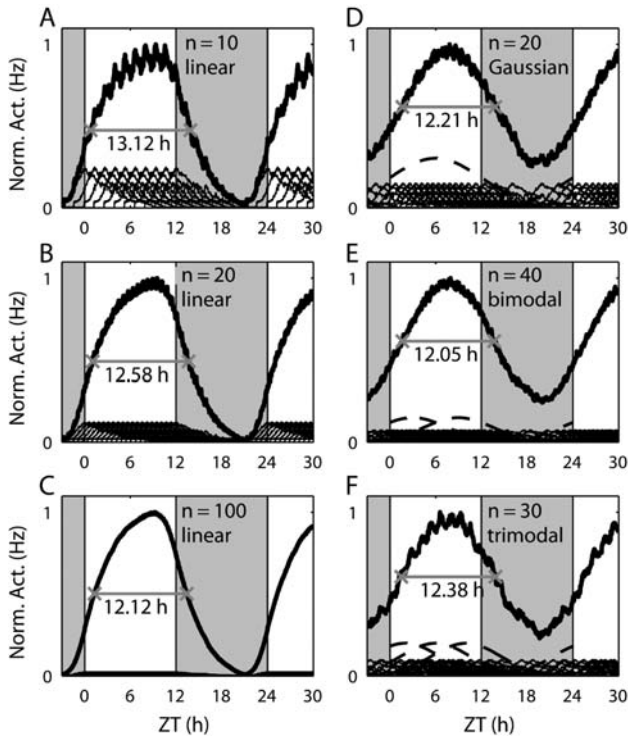
Figure 3. Multiunit activity pattern simulation for different numbers of single units and for several distributions. In A through C, single units are linearly distributed over the light period. In A, the summed activity of 10 single units is simulated; in B, 20 units are simulated; and in C, 100 units are simulated. The data indicate that an increment in the number of neurons affects the variability in the multiunit pattern but not the waveform. In D through F, the single units are distributed using different distributions. D shows 20 single units that are distributed using a normal (Gaussian) distribution over 24 h. The dashed line shows the Gaussian distribution according to which the single units are distributed. In E, the single units have a bimodal distribution with the mid of the first component at ZT3 and the mid of the second component at ZT9. The dashed lines show the Gaussian distribution of the 2 components. F shows a trimodal distribution with the mid of the 3 components at ZT2, ZT6, and ZT10. The data show that the multiunit waveform can be obtained by 3 temporal clusters of neurons. The data indicate that the multiunit waveform does not necessarily reflect the underlying distribution of single units.

Figure 4. Multiunit waveforms do not reflect the underlying distribution of single units. On the left-hand side, the distribution is shown of the subpopulations; on the right-hand side, the multiunit pattern resulting from this distribution is shown. (A) Two multiunit activity patterns of different subpopulations of neurons that are far apart in time result in a bimodal multiunit activity pattern. (B) Two multiunit activity patterns that are closer to each other result in a multiunit activity pattern with 1 peak. (C) Three multiunit activity patterns of different subpopulations may result in a multiunit activity pattern with 2 peaks. The data indicate that the multiunit activity pattern does not reflect the underlying distribution of subpopulations or single units.

distribution, broadening the single-unit activity pattern is not effective and, counterintuitively, leads to a narrower peak. The width of the multiunit pattern decreased from 13.32 h using narrow single-unit patterns to 13.12 h using the measured single-unit patterns and even to 12.45 h when broad single-unit patterns were used (Fig. 5B). We also investigated whether a change in phase relationship between the single-unit patterns can produce changes in the width of the multiunit pattern (Fig. 5C). Simulations show that the width of the multiunit pattern
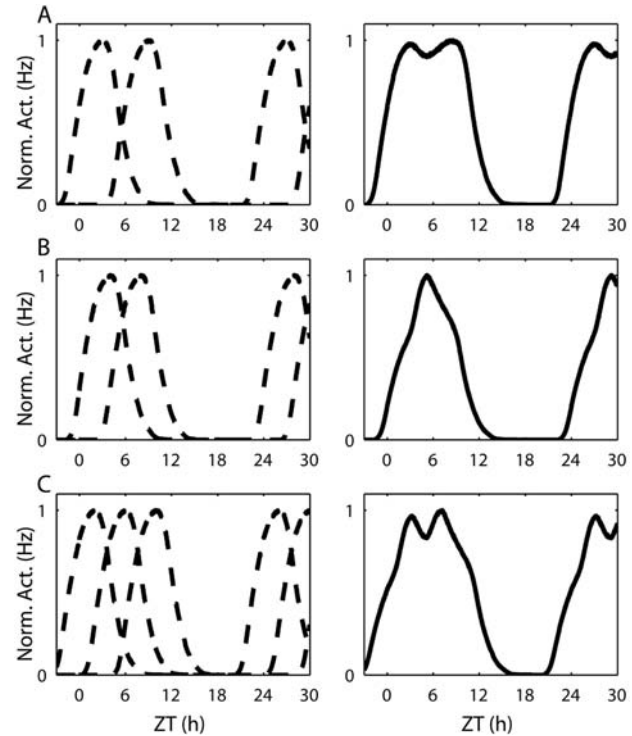
increased from 13.12 h on a normal day (LD 12:12) to 16.56 h on a long day, when the single units are linearly distributed over the long photoperiod. It decreased from 13.12 h to 9.38 h when the single-unit patterns were linearly distributed over the light period of a short day (LD 8:16; Fig. 5D).

Experimentally measured data show that the mean width of a multiunit pattern in a short photoperiod (LD 8:16) is 11.07 h, and in a long photoperiod (LD 16:8), it is 14.62 h (from Schaap et al., 2003). The difference between a long and short photoperiod is somewhat more than 3.5 h (Fig. 6A). We examined the effects of changes in the width of the single-unit pattern on the width of the multiunit pattern. The single-unit activity width ranged from near 0 up to 12 h (Fig. 6B). The results show that, counterintuitively, changes in single-unit activity patterns cannot code for
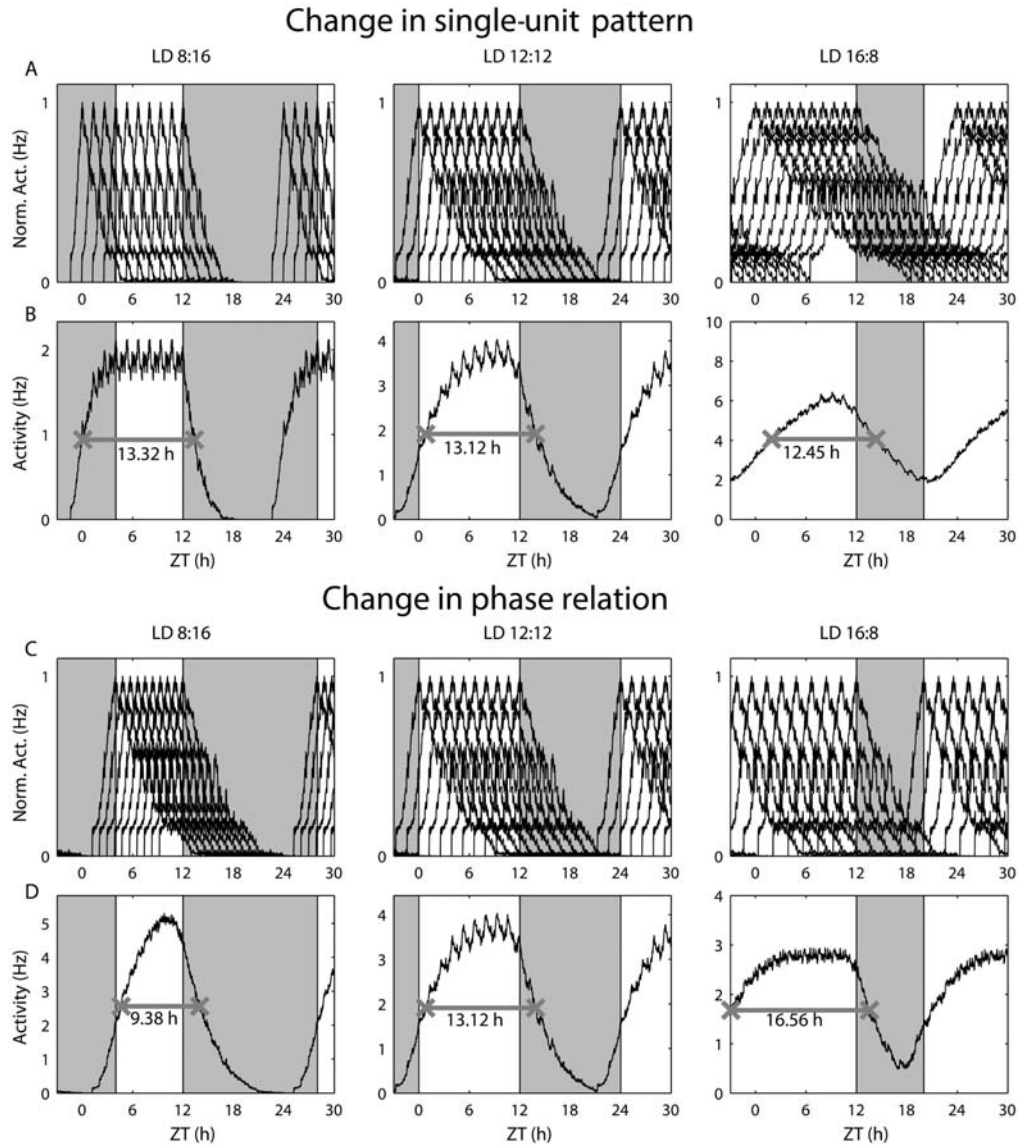
Figure 5.   Photoperiod encoding by changes in single-unit activity width or by changes in phase relations. For visualization, a linear distribution is used. (A) Phase distribution between the different single units remains the same, while the width of the single-unit activity pattern varies from a narrow pattern (half the width of a single-unit pattern) to encode for a short photoperiod to a broad pattern (twice the width of a single-unit pattern) to encode for a long photoperiod. (B) Simulated multiunit activity pattern corresponding to the single-unit width used in A. (C) Phase differences between the single units increase when the light period is extended. In a short photoperiod, the single units are distributed over a shorter time span than in the long photoperiod. (D) Simulated multiunit activity pattern corresponding to the distributions of single units used in C.

changes in multiunit pattern (measured at half-maximum amplitude) when single units are linearly distributed in phase. Instead, the linear distribution resulted in a decrease in multiunit pattern width when the single units became broader. For instance, a single-unit pattern with a width of 0.5 h resulted in a multiunit width of 12.65 h, while a single unit with a width of 10.5 h resulted in a multiunit width of 12.25 h for a given linear distribution. The Gaussian distribution showed a slight increase in multiunit width when the single-unit pattern was broadened. The predominant

increase in multiunit width occurred when a single-unit width of about 2 h (multiunit pattern width of 9.65 h) was lengthened to a single-unit width of about 6 h (multiunit pattern width of 11.08 h). This change in single-unit waveform resulted in an increase in multiunit width of less than 1.5 h.

A range of changes in phase relationship between single-unit patterns that are linearly distributed over the photoperiod resulted in considerable differences in the width of the multiunit pattern (Fig. 6C). For instance, when distributed over 8 h, the multiunit
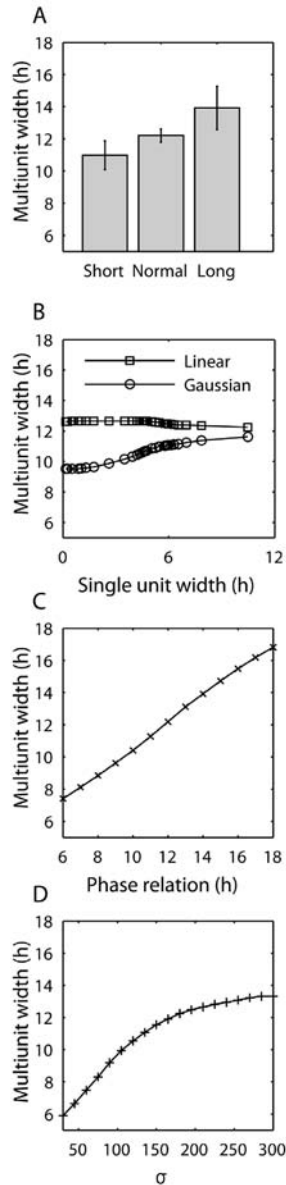
Figure 6. Photoperiod encoding using single-unit pattern width or phase distribution. (A) Experimental data from the rat SCN slice (± SEM) show that in a short photoperiod, the width of the multiunit pattern is narrower than in a long photoperiod (Schaap et al., 2003). B summarizes the effect of a change in width of the single-unit activity pattern on the width of the simulated multiunit pattern. On the *x*-axis, the width of the single units at halfmax is shown. The linear distribution shows that a narrow single-unit pattern results in almost the same simulated multiunit pattern width as a broad single-unit pattern. The normal distribution shows that a narrow pattern results in a somewhat smaller multiunit width than a broad pattern. C summarizes the effect of a change in phase relation of single-unit patterns on multiunit activity width for linear distributions. The *x*-axis indicates the range of the single units: in LD 12:12, the peaks of the single units are distributed over the 12-h light phase; in LD 16:8, the units are distributed over 16 h of light (see Fig. 5C). D shows the effect of changes in a normal (Gaussian) distribution on multiunit activity width using different values for σ. It is concluded that changes in phase relation can cause large changes in multiunit width, while changes in single-unit activity patterns have only minor effects.

pattern width was 8.85 h, and when distributed over 16 h, the multiunit pattern width was 15.49 h. This difference was about 6.5 h. For a Gaussian distribution, the σ indicates the width of the distribution. When a range of σs was used to alter the phase relationship between single units for the Gaussian distribution, significant differences in the width of the multiunit pattern were obtained (Fig. 6D). For instance, when σ is 105, the multiunit width was 9.95 h. A σ of 270 resulted in a multiunit width of 13.22 h. The difference between these 2 values is approximately 3.2 h.

Photoperiodic Encoding by 2 Populations

Bimodal distributions were characterized by the temporal distance between the 2 components and by the distribution of neurons within each of the components. We analyzed changes in distance between the 2 components (Figs. 7 A-D) and found that these lead to changes in multiunit patterns (Figs. 7 E-H). The pattern broadens if the components move away from each other, but when moved even further, the multiunit pattern shows 2 peaks.

For narrow single-unit distributions within a component, the system codes for photoperiod in the way expected: if the components are more separated, the multiunit activity pattern becomes broader (Fig. 8). This is true both for narrow normal distributions with σ values of 90, 120, and 150, which are relatively low (Fig. 8A), as well as for narrow linear distributions of 8 and 10 h (Fig. 8B). For broad distributions within a component (i.e., normal distributions with σ values of 180 and 210 or linear distributions of 14 and 16 h), the system codes for day-length opposite to the expectation: if the components are more separated, the multiunit activity pattern becomes narrower. To verify this, simulations were performed using the width of the population pattern at a fixed level of 8 Hz and at half-maximum amplitude. The results demonstrated that the summed waveform becomes narrower irrespective of the method used for determining the width (Fig. 9). If the components are separated 6 h, the width of the multiunit activity pattern is approximately 12 h, independent of the single-unit distribution that is used for each component.

DISCUSSION

In this study, we have simulated multiunit signals taken from distributed and nondistributed single units. The outcomes of the simulations were compared with
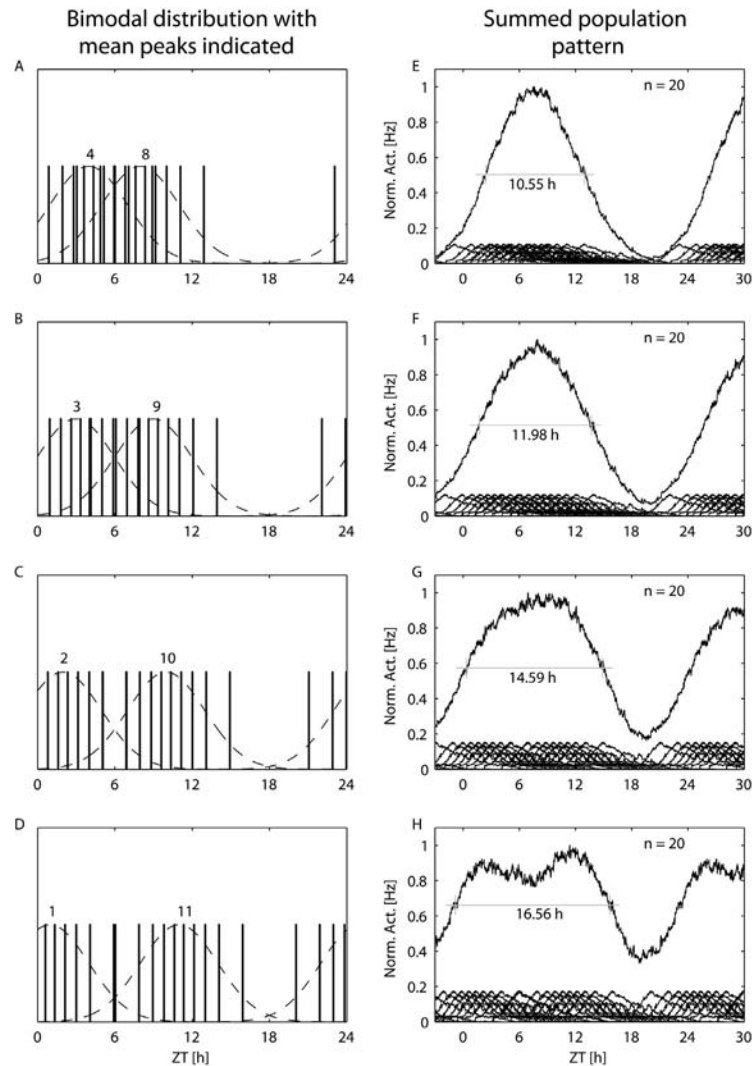
Figure 7. (A-D) Distribution of the 2 components in the circadian cycle. Two clusters in the bimodal distribution placed at different distances from each other. In A, the 2 components are 4 h apart; in B, they are 6 h apart; in C, the components are 8 h apart; and in D, the 2 components are 10 h apart. The numbers indicate the mean peak time for each component. The vertical lines indicate peak times of single units. The dashed lines indicate the distribution of single units within each cluster. The σ used for all the bimodal distributions is 90. **(E-H)** Multiunit activity patterns based on bimodal distributions used in A through D. In E, the 2 components are 4 h apart; in F, they are 6 h apart; in G, the components are 8 h apart; and in H, the 2 components are 10 h apart. We can see in H that if the clusters are too far apart, double peaks arise in the multiunit activity pattern. We conclude that a bimodal distribution can account for changes in multiunit patterns as observed under different photoperiods.

obtained experimental multiunit patterns. These recorded patterns were very precise and enabled us to evaluate them carefully for the presence of multiple components and the width of the multiunit pattern. The data show that realistic multiunit patterns can only be obtained when single units are distributed over the circadian cycle, in agreement with Schaap et al. (2003), who applied a linear distribution. In this study, the single units were distributed according to a linear, a Gaussian, a bimodal, and a trimodal distribution. We show that the outcome of all these simulations can render multiunit patterns that resemble the experimentally

recorded patterns. In other words, we show that solutions are possible for all distributions.

In the current simulations, we use a simplified model containing identical single-unit activity patterns. In reality, this may not be the case. The SCN is a heterogeneous structure, with respect to, among others, cell type, receptor density, neurotransmitter content, and afferent and efferent pathways (Morin and Allen, in press). A major differentiation appears to exist between the vasoactive intestinal polypeptide (VIP)–containing cells in the ventral SCN, which receive retinal afferents and the vasopressin-containing

Gaussian distribution
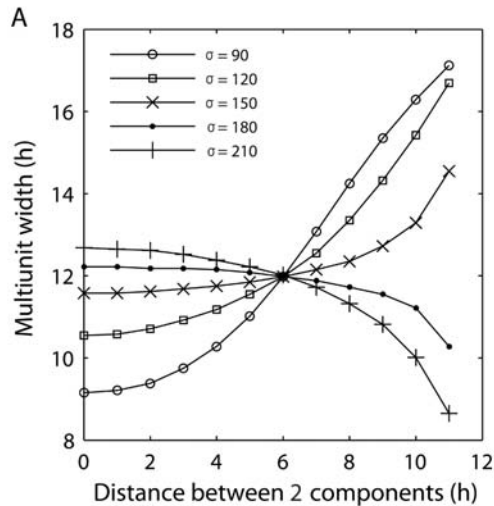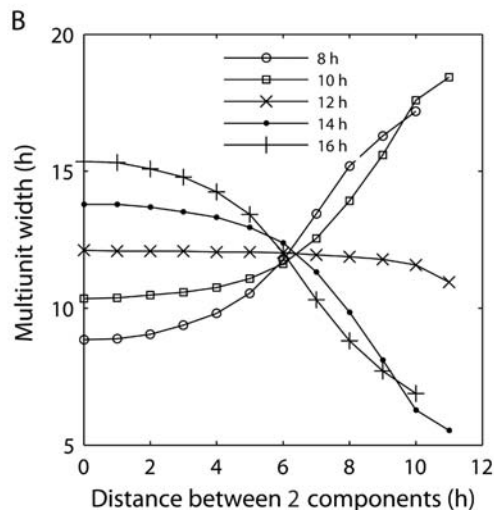
Linear distribution

Figure 8.   Effects of distance between components on multiunit width. On the *x*-axis, the temporal distance between both components is plotted; on the *y*-axis, the width of the multiunit activity pattern is plotted in hours. **(A)** Multiunit activity pattern width using a normal distribution within the components. The different σ values that are used represent the width of the Gaussian distribution that is used. A narrow Gaussian distribution has a small σ, while a broad distribution has a large σ. **(B)** Multiunit activity pattern width using a linear distribution for the single units within each component. The different lines represent different widths of these distributions. It can be observed that if the distance between both components is 6 h, the width of the multiunit activity pattern is always approximately 12 h. This is irrespective of the distribution that is used. For narrow distributions, the model codes for photoperiod in the way expected: if the components are more separated, the multiunit activity pattern becomes broader. This is the case in the normal distribution as well as in the linear distribution. For broad distributions, the model counterintuitively codes for photoperiod exactly opposite to the narrow distributions: if the components are more separated, the multiunit activity pattern becomes narrower.

cells in the dorsal SCN (Moore and Silver, 1998; van den Pol, 1980). It may well be that heterogeneity relates to differences in single-unit activity patterns or that within particular regions of the SCN, units show different circadian profiles. This cannot be incorporated in the present simulations but is an interesting possibility for future simulations, if experimental data will point in this direction. Despite the present uncertainty about the differences in single-unit activity patterns within the SCN, it has become clear that all recorded single-unit activity patterns are considerably narrower than the multiunit pattern and show differences in phase (Schaap et al., 2003; Brown et al., 2005). These narrow single-unit patterns, as well as the phase differences among the neurons, were the major and sole assumption for the present simulations.

Of note, single-unit activity patterns from isolated neurons may deviate from patterns in a network, not only with respect to their cycle-to-cycle precision (Herzog et al., 2004; Honma et al., 1998) but also with respect to the broadness of their activity patterns. The present simulations were not designed to provide insight in coupling mechanisms (i.e., phase response relations) between neurons (see Kunz and Achermann, 2003) but aimed to provide insight in the relation between the behavior of individual neurons and the measured population activity. The starting point in these simulations is the recorded activity pattern of a neuron in a network that had presumably been shaped by the interactions with other neurons.

The simulations indicate that the phase distribution of single-unit activity patterns cannot be derived from the multiunit activity pattern. For instance, a bimodal distribution of single units may show up as a bimodal multiunit pattern if the components are temporally far enough apart but may show up as a unimodal distribution when closer in phase. We also showed that a trimodal distribution can result in bimodal multiunit patterns. This shows that single-unit recordings are required to establish how the SCN multiunit patterns are determined by the individual oscillatory cells, their individual patterns, and their phase relation.

While the present simulations were based on electrical activity recordings, the simulations also have relevance for other population measurements such as gene expression profiles, transmitter concentrations, and so on. It will be important to establish whether molecular expression profiles of individual neurons resemble the population pattern or show short periods of enhanced expression within the 24-h cycle, with peaks at different phases of the circadian cycle.
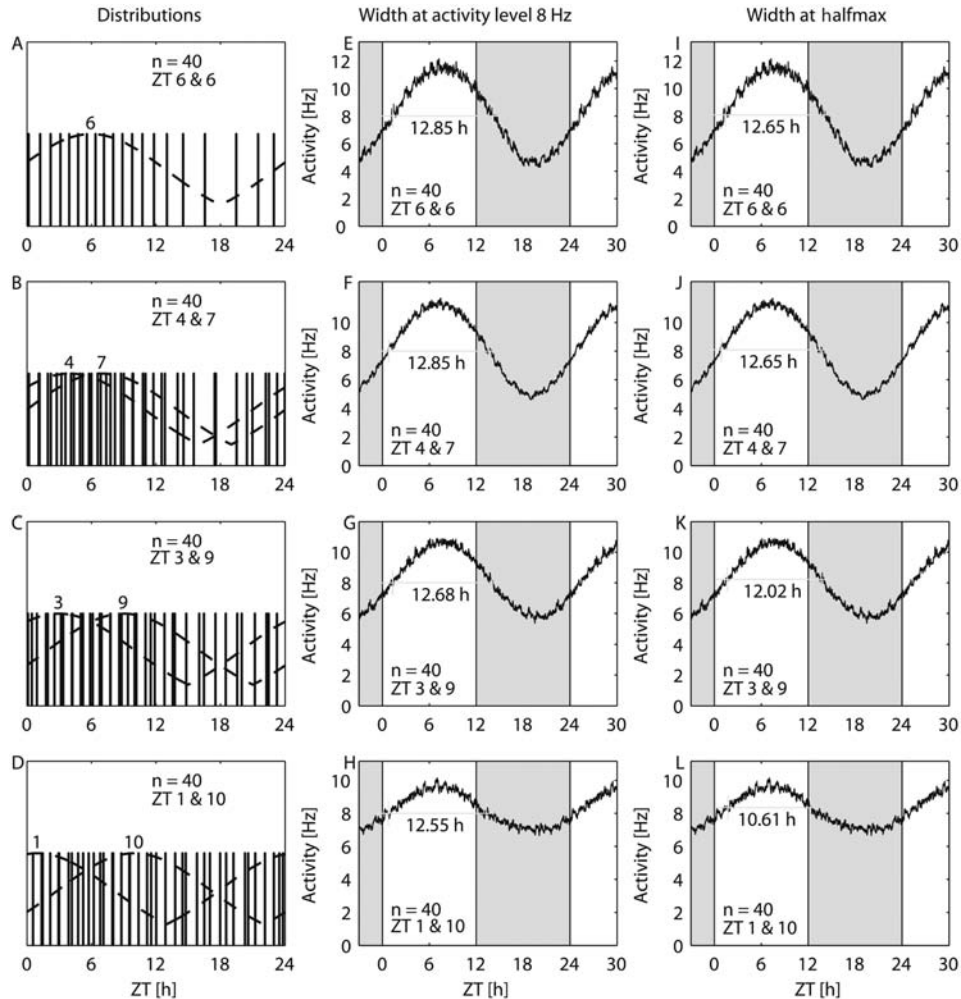
Figure 9. Distribution of the 2 components in the circadian cycle and their effect on the population width. (A-D) Two clusters in the bimodal distribution are placed at different distances from each other. In A, the 2 components are on top of each other; in B, C, and D, the components are 3, 6, and 9 h apart, respectively. The vertical lines in A through D indicate peak times of single units. The dashed lines indicate the distribution of single units within each cluster. The σ used for all the bimodal distributions is 210, which is a broad distribution. (E-H) Multiunit activity patterns based on bimodal distributions used in A through D, measured at a constant height of 8 Hz. (I-L) Multiunit activity patterns based on bimodal distributions used in A through D, measured at half-maximum height. It is obvious that the summed waveform is narrower, at half-maximum width, and also at a particular activity level, when the 2 components are further apart.

The observation that neurons show out of phase oscillations in Per1 (Quintero et al., 2003; Yamaguchi et al., 2003) may indicate that phase differences also exist at the molecular level and may play a significant role in adjustments of molecular cycles to different environmental conditions.

When the number of neurons is increased in the simulations, the width of the multiunit pattern remains relatively stable. However, when more neurons are incorporated, the multiunit pattern becomes smoother and more precise. Mathematical modeling of multiunit activity in neuronal networks has shown that an increment in the number of neurons results in increased precision (i.e., decrease in day-to-day

variability) at the multiunit level (Enright, 1980). Noteworthy, increased precision in the latter model results from a stochastic process in which the ensemble pattern of imprecise neurons renders accuracy at the network level.

Herzog et al. (2004) and Honma et al. (1998) confirm that single neurons have imprecise periods but also state that precision is enhanced when neurons synchronize in a network, such as in a slice. Quintero et al. (2003) found in slices that a variation in period exists between neurons but are uncertain about differences in period within a neuron. Yamaguchi et al. (2003) suggest that intrinsic network properties could give rise to fixed phase relations between neurons.

However, intrinsic network properties may also result in variable phase relations (i.e., when coupling is weaker or when afferent pathways are stimulated). The variations in period, either between or within neurons, may underlie the observed phase differences between SCN neurons (Schaap et al., 2003; Brown et al., 2005). In our simulations, single units were given a fixed period, and as a result, they peak at a fixed phase of the circadian cycle. However, the outcome of the simulations would be similar if an earlier neuron on day 1 becomes a later neuron on day 2 while another neuron behaves vice versa, as long as the overall phase distribution between neurons is preserved.

Photoperiodic Encoding

Our simulations revealed that changes in phase relations between single units can better account for photoperiodic encoding by the SCN than changes in the single-unit activity patterns themselves. We also observed that changes in phase are more effective in a linear distribution than in a normal distribution. Although the linear distribution is unlikely in a biological process, it could represent a multitude of components within the SCN that are evenly distributed over the subjective day. The trimodal distribution was not analyzed in photoperiodic simulations but is consistent with components that are about 4 h apart from one another (Quintero et al., 2003; Meijer et al., 1997).

At this stage, it is unknown to what extent single-unit patterns change under different day-lengths, nor do we know whether the changes in phase relation that were selected in the present simulations are realistic. Nevertheless, it is shown that extensive changes in single-unit activity patterns lead to only minor changes in multiunit activity patterns, whereas relatively small changes in phase distribution among individual neurons have considerable effect on the multiunit waveform. In a linear distribution, broadening of the single-unit activity pattern counterintuitively leads to a decrease in multiunit width. An explanation is that for broader single units, the trough of the multiunit pattern increases, as the descending part of the previous cycle will overlap with the increasing part of the following cycle. A different method of calculating the multiunit pattern width (i.e., measuring at half-maximum height) will give rise to other results. Nevertheless, increments in phase relationship between oscillatory cells yield an increase in population waveform, irrespective of the

way in which the population pattern width is calculated. In a Gaussian distribution, changing the width of the single units from 2 to 6 h resulted in an increment in the multiunit width of 1.5 h. This increment is relatively small as compared to the substantial change in single-unit patterns. We conclude that changes in the phase relationship between neurons are an effective mechanism by which SCN neurons can code for day-length.

Thus far, all conclusions were based on normalized discharge patterns, in which the maximum frequency was equaled to 1. When we analyze the discharge levels quantitatively and study changes in discharge levels that follow from different parameter settings, we observe that for phase changes between the single units, the maximal frequency of the multiunit pattern decreases somewhat in a long day-length and increases in a short day (Fig. 5D). For instance, in Figure 5, the multiunit activity for long day-lengths decreases to about 56% of the activity for short day-lengths. These effects should be measurable and are, in fact, consistent with multiunit recordings in the rat by Schaap et al. (2003).

Changes in width of the single-unit activity pattern lead to major changes in total SCN activity (Figs. 5 A and B). For instance, an increase in single-unit width from 2 to 6 h—required to increase the multiunit peak by 1.5 h in a normal distribution—would lead to a substantial (about 3-fold) increase in the multiunit activity level (from 2 to 6 Hz in Fig. 5). These changes in impulse frequency are not apparent from recordings in rats and hamsters (Mrugala et al., 2000; Schaap et al., 2003). However, as the number of counted neurons also depends on spike trigger settings and electrode characteristics, this conclusion needs further confirmation.

The present results are important for the design of future experiments. When photoperiodic encoding results from adaptations in single-unit activity, relatively large changes in single-unit activity patterns are predicted. These should be easy to record, and the number of neurons or animals that should be recorded from need not be large. Moreover, multiunit activity patterns should not only broaden in long day-lengths, but the maximum frequency should also increase. If alterations in phase distributions are the mechanism for photoperiodic encoding, the frequency of the multiunit activity peak in long days should decrease. In addition, single units should reveal a larger distribution in phase. It is difficult to predict how many recordings will be required to confirm the latter point.

Bimodal Distributions

The 2-component structure of the SCN pacemaker, also called E (evening) and M (morning) oscillators, plays a significant role in a vast amount of literature in the field of circadian rhythms (Pittendrigh and Daan, 1976; Daan and Berde, 1978; Daan et al., 2001; Hastings, 2001; Illnerova and Vanecek, 1982; Sumova et al., 1995). For this reason, we also explored bimodal distributions in our simulations. In terms of our current work, the 2-oscillator model is a specific version of a model in which phase distribution determines day-length encoding. We found that bimodal distributions can encode for day-length but that this is not trivial. Instead, and to our surprise, 2 components can code for day-length only when certain conditions are met. The first is evidently that the 2 components should move within the right boundaries. While small movements yield no effect on multiunit waveform, the pattern becomes bimodal when the components are moved too far apart.

The system will only function properly if not only the distance between the components is taken into consideration but also the distribution within a component. The latter restriction has not been acknowledged before. Only if both components have relatively small distributions of single units can the resulting multiunit pattern encode for day-length. If the distributions of single units are broad for both components, moving the peaks of the 2 components apart results, against the expectation, in a narrower multiunit pattern. Additional simulations showed that the summed waveform is more narrow, not only at half-maximum width but also at a particular activity level (Fig. 9). In a bimodal distribution, neurons within each component are commonly distributed according to a Gaussian distribution. We also used a linear distribution of neurons within each component and show that this leads to the same results. We conclude that 2 components can code for day-length when specific conditions are met. Hence, the 2-oscillator model is a possible but not self-evident option for day-length encoding. Of note, the temporal distribution within the SCN may or may not be related to a spatial distribution. There may be 2 areas with out-of-phase neurons, depending on the environmental condition (anterior-posterior: Hazlerigg et al., 2005; dorsal-ventral: Albus et al., 2005; de la Iglesia et al., 2004). Bimodality in phase may theoretically also arise in a more diffuse way in which earlier and later neurons are intermingled in the SCN.

In conclusion, it has been observed that single-unit activity patterns deviate from the population pattern of the SCN (Schaap et al., 2003; Brown et al., 2005). This implies that single units do not mirror image the population activity pattern. To understand the relation between single-unit and multiunit data, simulations are conspicuously suited. A simulation model in which it is possible to simulate a multitude of possible configurations can help in understanding the multioscillator structure of the SCN.

REFERENCES

Albus H, Vansteensel MJ, Michel S, Block GD, and Meijer JH (2005) A GABAergic mechanism is necessary for coupling dissociable ventral and dorsal regional oscillators within the circadian clock. Curr Biol 15:886-893.

Brown TM, Hughes AT, and Piggins HD (2005) Gastrin-releasing peptide promotes suprachiasmatic nuclei cellular rhythmicity in the absence of vasoactive intestinal polypeptide-VPAC2 receptor signaling. J Neurosci 25:11155-11164.

Daan S, Albrecht U, Van der Horst GTJ, Illnerova H, Roenneberg T, Wher TA, and Schwartz WJ (2001) Assembling a clock for all seasons: Are there M and E oscillators in the genes? J Biol Rhythms 16:105-116.

Daan S and Berde C (1978) Two coupled oscillators: Simulations of the circadian pacemaker in mammalian activity rhythms. J Theor Biol 70:297-313.

de la Iglesia HO, Cambras T, Schwartz WJ, and Diez-Noguera A (2004) Forced desynchronization of dual circadian oscillators within the rat suprachiasmatic nucleus. Curr Biology 14:796-800.

Enright JT (1980) *The Timing of Sleep and Wakefulness: On the Substructure and Dynamics of the Circadian Pacemakers Underlying the Wake-Sleep Cycle*. Berlin: Springer Verlag.

Hastings M (2001) Modeling the molecular calendar. J Biol Rhythms 16:117-123.

Hazlerigg DG, Ebling FJP, and Johnston JD (2005) Photoperiod differentially regulates gene expression rhythms in the rostral and caudal SCN. Curr Biol 15:R449-R450.

Herzog ED, Aton SJ, Numano R, Yoshiyuki S, and Tei H (2004) Temporal precision in the mammalian circadian system: A reliable clock from less reliable neurons. J Biol Rhythms 19:35-46.

Honma S, Nakamura W, Shirakawa T, and Honma K (2004) Diversity in the circadian periods of single neurons of the rat suprachiasmatic nucleus depends on nuclear structure and intrinsic period. Neurosci Lett 358:173-176.

Honma S, Shirakawa T, Katsuno Y, Namihira M, and Honma K (1998) Circadian periods of single suprachiasmatic neurons in rats. Neurosci Lett 250:157-160.

Illnerova H and Vanecek J (1982) Two-oscillator structure of the pacemaker controlling the circadian rhythm of N-acetyltransferase in the rat pineal gland. J Comp Physiol 145:539-548.

Jac M, Kiss A, Sumova A, Illnerova H, and Jezova D (2000) Daily profiles of arginine vasopressin mRNA in the suprachiasmatic, supraoptic and paraventricular nuclei of the rat hypothalamus under various photoperiods. Brain Res 887:472-476.

Jagota A, de la Iglesia HO, and Schwartz WJ (2000) Morning and evening circadian oscillations in the suprachiasmatic nucleus in vitro. Nat Neurosci 3:372-376.

Kunz H and Achermann P (2003) Simulation of circadian rhythm generation in the suprachiasmatic nucleus with locally coupled self-sustained oscillators. J Theor Biol 224:63-78.

Meijer JH, Schaap J, Watanabe K, and Albus H (1997) Multiunit activity recordings in the suprachiasmatic nuclei: In vivo versus in vitro models. Brain Res 753:322-327.

Moore RY and Silver R (1998) Suprachiasmatic nucleus organization. Chronobiol Int 15:475-487.

Morin LP and Allen CN (In press) The circadian visual system, 2005. Brain Res Brain Res Rev.

Mrugala M, Zlomanczuk P, Jagota A, and Schwartz WJ (2000) Rhythmic multiunit neural activity in slices of hamster suprachiasmatic nucleus reflect prior photoperiod. Am J Physiol Regulatory Integrative Comp Physiol 278: R987-R994.

Pittendrigh CS and Daan S (1976) A functional analysis of circadian pacemakers in nocturnal rodents: V. pacemaker structure: A clock for all seasons. J Comp Physiol 106:333-355.

Quintero JE, Kuhlman SJ, and McMahon DG (2003) The biological clock nucleus: A multiphasic oscillator network regulated by light. J Neurosci 23:8070-8076.

Schaap J, Albus H, vanderLeest HT, Eilers PHC, Détári L, and Meijer JH (2003) Heterogeneity of rhythmic suprachiasmatic nucleus neurons: Implications for circadian waveform and photoperiod encoding. PNAS 100:15994-15999.

Schwartz WJ, de la Iglesia HO, Zlomanczuk P, and Illenrova H (2001) Encoding *Le Quattro Stagioni* within the mammalian brain: Photoperiodic orchestration through the suprachiasmatic nucleus. J Biol Rhythms 16:302-311.

Shinohara K, Honma S, Katsuno Y, Abe H, and Honma K (1995) Two distinct oscillators in the rat suprachiasmatic nucleus in vitro. Proc Natl Acad Sci USA 92:7396-7400.

Sumova A, Travnickova Z, Peters R, Schwartz WJ, and Illnerova H (1995) The rat suprachiasmatic nucleus is a clock for all seasons. Proc Natl Acad Sci USA 92: 7754-7758.

van den Pol AN (1980) The hypothalamic suprachiasmatic nucleus of rat: Intrinsic anatomy. J Comp Neurol 191:661-702.

Watanabe K, Koibuchi N, Ohtake H, and Yamaoka S (1993) Circadian rhythms of vasopressin release in primary cultures of rat suprachiasmatic nucleus. Brain Res 624:115-120.

Welsh DK, Logothetis DE, Meister M, and Reppert SM (1995) Individual neurons dissociated from rat suprachiasmatic nucleus express independently phased circadian firing rhythms. Neuron 14:697-706.

Yamaguchi S, Isejima H, Matsuo T, Okura R, Yagita K, Kobayashi M, and Okamura H (2003) Synchronization of cellular clocks in the suprachiasmatic nucleus. Science 302:1408-1412.